SHEAR BEHAVIOR OF HIGH STRENGTH CONCRETE BEAMS REINFORCED BY GFRP AND STEEL BARS

Youssef H. Hammad[1], Ibrahim G. Shaaban[2], Ibrahim M. Bazzan[3] and Walid H. Awwad[4]
[1] Professor of Reinforced Concrete Structures, [2] Associate Professor, [3] Assistant Professor and [4] Graduate Student
Civil Engineering Department, Faculty of Engineering, Shoubra, Zagazig University

ABSTRACT

Ten simply supported reinforced concrete T-beams were experimentally tested under two symmetrically concentrated loads. Nine of the studied beams were made of High Strength Concrete (HSC) with mean compressive strength 70 N/mm² while the control beam was made of normal strength concrete (NSC) with compressive strength 30 N/mm². Five of the studied beams were reinforced by High Tensile Steel (HTS) bars and the other four specimens were reinforced by Glass Fiber Reinforced Plastics (GFRP) bars. The control beam was reinforced by HTS bars as main reinforcement. The web reinforcement for all the test beams was in the form of vertical stirrups. All beams were designed according to the provisions of ACI 318-99. The studied parameters were the amount of web reinforcement, shear span to depth ratio (a/d) and type of main reinforcement (GFRP and HTS). The actual shear strength of each beam was compared with the strength predicted by different codes of practice such as ACI 318-99, BS-8110, and ECCS 203-2001in order to establish an empirical formula for the analysis and design of HSC beams reinforced with GFRP bars. Within the limits of the test results of this research, it was found that increasing a/d from 1.5 to 3.5 resulted in reducing the ultimate capacity of the studied beams of approximately 42%. In addition, increasing the amount of web reinforcement μv from 0.202 to 0.324 resulted in increasing the ultimate capacity of the studied beams by approximately 53%. Moreover changing the type of main reinforcement from HTS to GFRP, while keeping the reinforcement ratio constant at $\mu=0.58\ \mu b$, resulted in a great reduction of the ultimate capacity of the studied beams.
Keywords: *High-Strength Concrete, Shear Reinforcement, Shear Strength, GFRP, Reinforced Concrete, T-Beams, Analysis And Design.*

INTRODUCTION

In shear, beams mainly fail abruptly without advanced warning and the developed diagonal cracks are considerably wider than flexural cracks [1]. To avoid such abrupt shear failure, adequate amounts of shear reinforcement are required. Shear strength of reinforced concrete beams is dependent on several factors including concrete compressive strength, amount of longitudinal steel, shear span to depth ratio, size effect, residual tensile stresses transmitted directly across cracks and provisions of web reinforcement [2]. Recently, production of HSC of compressive strength approaching (130 MPa) has been used in cast in place with conventional methods of production by reducing the water cement ratio, specifying fine and coarse aggregate and adding silica fume and super plasticizers [3]. One feature of HSC is the tendency of cracks to pass through instead of around the aggregates. This creates smoother crack surfaces and

reduces the aggregates interlock. As a result, higher dowel forces occur in the longitudinal reinforcing bars. These higher dowel forces, together with the highly concentrated bond stresses in HSC beams result in higher bond splitting stresses where the shear cracks cross the longitudinal tension bars. This effect leads to brittle shear failures. The inclusion of an appropriate amount of minimum shear reinforcement can control these horizontal splitting cracks and result in improving shear response [4]. Most of the major concrete codes are based on researches conducted on structural members made of NSC. Recently, some of concrete codes have included provisions for the design of HSC members. Extrapolations of NSC design rules to be used for HSC may not be always appropriate. If the mode of failure was brittle, as with shear failure, extrapolating existing NSC design rules for use with HSC may result in less or non- conservative design criteria [5].

The use of fiber reinforced plastic (FRP) reinforcing bars to replace steel reinforcing bars has emerged as one of the many techniques to enhance the corrosion resistance of reinforced concrete structures [6]. Nawy and Neuwerth [7] found that the reinforcing ratio of FRP in concrete beams reinforced with GFRP bars did not affect moment capacity because the beams failed by crushing of concrete in the compression zone. Saadatmanesh and Ehsani [8] studied concrete beams reinforced longitudinally with different combinations of GFRP and steel reinforcing bars with web reinforcement. They found that specimens reinforced with FRP stirrups and steel longitudinal reinforcement failed as a result of yielding in the longitudinal bars. Satoh et al [9] found that the failure load can be calculated using elastic theory for concrete beams reinforced with different type of fiber reinforcement such as armid, carbon, glass and D13 steel fiber reinforcement. Faza and GangaRao [10] reported that HSC must be used instead of NSC for concrete beams reinforced with GFRP reinforcing bars in order to take advantage of the high ultimate strength of FRP reinforcing bars. Zia et al [11] found that no shear failure was developed for concrete beams reinforced with FRP bars but the beams failed due to tensile rupture of the longitudinal FRP bars.

The present investigation is a part of a larger research performed to study the shear behavior of HSC beams reinforced by GFRP with different web reinforcement and shear span to depth ratio [12]. The main objective was to study the effect of using GFRP as longitudinal reinforcement in HSC beams on the cracking behavior, load carrying capacity, modes of failure, load deflection response, and strain in reinforcing bars. In addition, an empirical formula was developed for the analysis and design of HSC beams reinforced with GFRP as main reinforcement.

TEST PROGRAM AND EXPERIMENTAL WORK

Test Specimens

The test program consisted of ten simply supported reinforced concrete beams with web reinforcement in the form of vertical stirrups. All the studied beams were T-shaped in cross section as shown in Figure 1. Table 1 shows a description of the test beams along with the studied parameters and the actual cube compressive strength for the different specimens. The main reinforcement ratio in all the test beams was kept constant of (μ=0.58 μb), which was recommended by ACI 318-99 [13] for R.C beams reinforced by HTS. Two different mixes were used to develop normal and high strength concrete at 28 days of target strength 30 and 70 N/mm², respectively. Table 2 shows the mix designs for the two concrete strengths. The used GFRP bars were fabricated from vinyl ester with an outer coat to seal the bar. The bar is produced using drown continuous "C "glass rovings and has a longitudinal irregular surface. A single strand spiral wrap around the outside diameter produces a spiral indentation in the bar. The properties of the GFRP bars were given by the producing factory [14].

Table 1 Description of Test Beams and Studied Parameters

Beam	f_{cu}	$\mu s = As/bd$	As	$\mu v = Av/bS$	No. Of stirrups	a/d
B1	30	2.83 % (H.T.S)	4 Φ 12	0.202	¢6 @ 280 mm	2.5
B2	68.8	3.93 % (H.T.S)	2 Φ 16 + 2 Φ 12	0.202	¢6 @ 280 mm	1.5
B3	68.8	3.93 % (H.T.S)	2 Φ 16 + 2 Φ 12	0.202	¢6 @ 280 mm	2.5
B4	67.5	3.93 % (H.T.S)	2 Φ 16 + 2 Φ 12	0.202	¢6 @ 280 mm	3.5
B5	69.2	3.93 % (H.T.S)	2 Φ 16 + 2 Φ 12	0.324	¢6 @ 175 mm	2.5
B6	67.5	3.93 % (H.T.S)	2 Φ 16 + 2 Φ 12	0.50	¢8 @ 200 mm	2.5
B7	71.2	0.53% (GFRP)	3 ¢ 6	0.202	¢6 @ 280 mm	1.5
B8	71.4	0.53% (GFRP)	3 ¢ 6	0.202	¢6 @ 280 mm	2.5
B9	67.7	0.53% (GFRP)	3 ¢ 6	0.324	¢6 @ 175 mm	2.5
B10	71.5	0.53% (GFRP)	3 ¢ 6	0.202	¢6 @ 280 mm	3.5

f_{cu} = average cube compressive strength of concrete, N/mm².
μs = longitudinal reinforcement ratio, As/bd.
μv = web reinforcement ratio, Av/(bS) %.
Φ = bar diameter, high tensile steel, mm. & ¢ = bar diameter, ordinary mild steel, mm.
¢ = bar diameter, GFRP bars, mm.
a/d = shear span to depth ratio.

Table 2 Concrete Mix-Design

Mix No.	Cement kN	Sand kN	Crushed Basalt kN	Silica fume kN	Water Kn	Superplasticizer kN
1	3.50	6.40	11.80	---	1.80	---
2	5.50	5.50	11.25	0.80	1.60	0.23

Test Procedure

Each beam was tested as simply supported beam under two vertical concentrated loads by using two vertical hydraulic jacks which were similar in their acting position and value. The vertical loads were applied in increments (20 kN for beams reinforced by HTS and 5 kN for beams reinforced by GFRP). After each increment, the strains in the main steel and stirrups were measured using electrical strain gauges of length 5 mm, resistance 120.4 ± 0.4 ohm, and a gauge factor of 2.11. Detection of cracks and marking them for each incremental load were made when the load reached its steady state. Figure 2 shows a typical studied beam during testing.
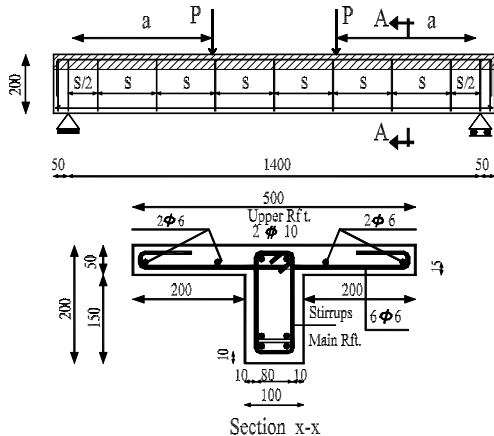

Fig. 1 Details of test beams.

Fig. 2 Test setup of a typical test beam

ANALYSIS AND DISCUSSION OF THE TEST RESULTS

Cracking Pattern and Failure Mode

Figure 3 shows the cracking pattern and failure mode for all test beams. Cracking load, ultimate load capacity and modes of failure for the test beams are listed in Table 3. Generally, the first crack for all beams occurred in the flexural region perpendicular to the direction of the maximum principal stress induced by pure moment. It was noticed that with increasing the load, the shear stresses become more important and induced inclined cracks. The cracks propagated, spread and widened due to the effect of combined shear and bending stresses. Cracks formation for beams from B1 through B6 (beams reinforced with HTS) gradually developed as the load increased. Approaching the failure load level, shear cracks started from the support and propagated diagonally towards the point load. For beams from B7 through B10 (beams reinforced with GFRP) formation of cracks was sudden along the depth of the beams. Similar observations were found by Benmokrane et al [6] and Masmoudi et al [15]. At failure load, both of the flexural cracks and the diagonal shear ones spread into small cracks in the lower third of the beam web in a shape like tree roots (see Figure 3). These small cracks were connected horizontally to form horizontal splitting cracks at the level of the longitudinal main reinforcement.

It can be seen from Figure 3 that increasing a/d lead to more cracks concentrated in the flexural region. On the other hand, decreasing a/d resulted in distributing the cracks uniformly all over the length of the beam. Figure 3 shows also that when the web reinforcement increased (for beams B5, B6 and B9) the cracks spacing decreased while the number of cracks and crack width increased. Johnson and Ramirez [16] and Abdoun [17] recorded similar observations in their studies. Figure 3 and Table 3 show that changing the type of main reinforcement from HTS (B1 to B6) to GFRP (B7 to B10) lead to changing the failure mode from diagonal tension shear failure to flexural failure. This may be attributed to the fact that beams reinforced with GFRP rods showed no yielding and hence deflection continued as the load increased. It was observed that for beams reinforced with GFRP rods, the crack width was wider and the crack spacing was narrower due to the low modulus of elasticity of GFPR rods compared with HTS ones. This is in agreement with the observations of Benmokrane et al [6]. When the load was released, recovery of the cracks with a reduction of deflection and width of cracks were noticed. It can be argued that the GFRP rods are elastic and the release of loading lead to such recovery of the cracks.

Table 3 Measured Cracking and Maximum Shear Load of the Test Beams

Beam	F_{cu}	As	No. Of stir.	a/d	P_{cr}	P_f	Failure Mode
B1	30	4 Φ 12	¢6 @ 280 mm	2.5	30.0	102.0	Diagonal Tension
B2	68.8	2 Φ 16 + 2Φ12	¢6 @ 280 mm	1.5	65.0	270.0	Diagonal Tension
B3	68.8	2 Φ 16 + 2Φ12	¢6 @ 280 mm	2.5	50.0	188.0	Diagonal Tension
B4	67.5	2 Φ 16 + 2Φ12	¢6 @ 280 mm	3.5	17.5	150.0	Diagonal Tension
B5	69.2	2 Φ 16 + 2Φ12	¢6 @ 175 mm	2.5	40.0	200.0	Diagonal Tension
B6	67.5	2 Φ 16 + 2Φ12	¢8 @ 200 mm	2.5	20.0	215.0	Diagonal Tension
B7	71.2	3 ¢ 6	¢6 @ 280 mm	1.5	17.5	60.0	Flexural Tension
B8	71.4	3 ¢ 6	¢6 @ 280 mm	2.5	15.0	42.5	Flexural Tension
B9	67.7	3 ¢ 6	¢6 @ 175 mm	2.5	17.5	65.0	Flexural Tension
B10	71.5	3 ¢ 6	¢6 @ 280 mm	3.5	10.0	35.0	Flexural Tension

P_f = failure load (kN). & P_{cr} = cracking load (kN).

<div align="center">(B1)</div> <div align="center">(B2)</div>

<div align="center">(B3)</div> <div align="center">(B4)</div>

<div align="center">(B5)</div> <div align="center">(B6)</div>

<div align="center">(B7)</div> <div align="center">(B8)</div>

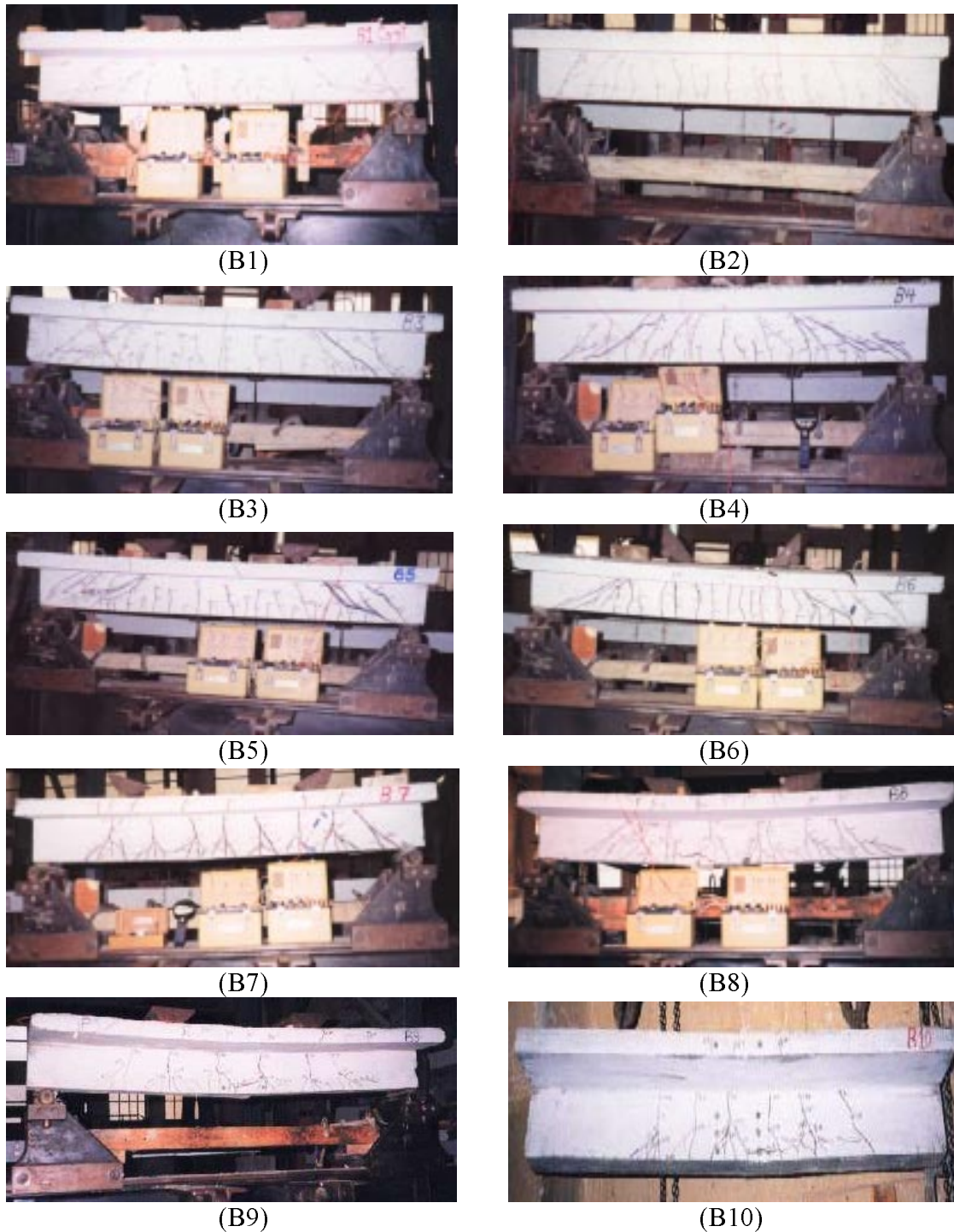<div align="center">(B9)</div> <div align="center">(B10)</div>

Fig. 3 Crack patterns of test beams.

Load Deflection Response

The effects of the studied parameters such as shear span to depth ratio, the amount of web reinforcement and type of main reinforcement (GFRP and HTS) on the load deflection relationship of the studied beams were illustrated in Figures 4 to 6. Figure 4 shows that increasing a/d from 1.5 for Beam B7 to 2.5 for Beam B8 lead to a reduction in the ultimate load by approximately 29%. In addition, the slope of the load-deflection curve reduced from 44.11 kN/mm to 35.71 kN/mm and the deflection increased by 15%. Further reduction of the ultimate load took place by increasing a/d

to 3.5 for beam B10 (by approximately 42%), the slope of the load-deflection curve reduced from 44.11 kN/mm to 25.86 kN/mm and the deflection increased by 42%. The same trend was observed by Abdoun [17] for HSC beams reinforced by HTS main reinforcement. Figure 5 shows that increasing μv from 0.202 for beam B8 to 0.324 for B9 resulted in a slight change in the behavior of such beams. The ultimate load increased by approximately 53%, the slope of the load-deflection curve slightly reduced from 35.71 kN/mm to 34.09 kN/mm and the maximum deflection increased by approximately 16%. Figures 4 and 5 show that the effect of a/d is more significant than that of changing μv ratio for HSC beams reinforced by GFRP rods.
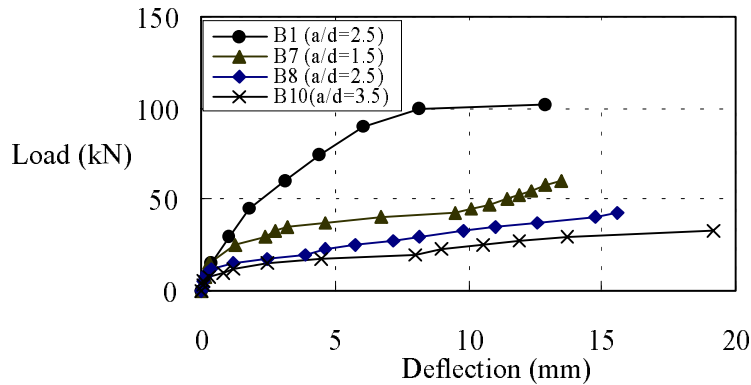

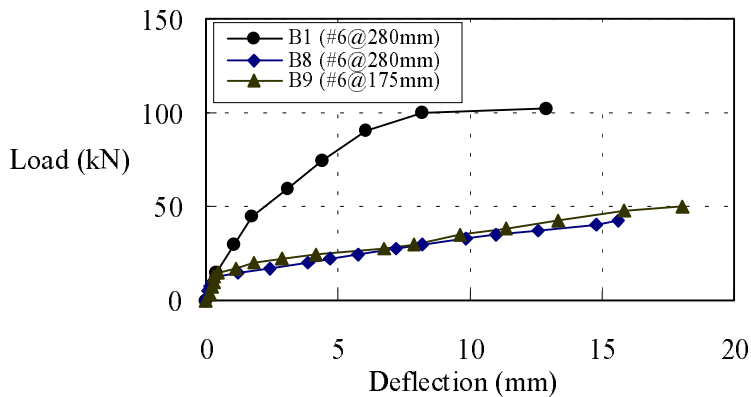Fig. 4 Effect of (a/d) on the load-deflection relationship.

Fig. 5 Effect of (μv) on the load-deflection relationship.
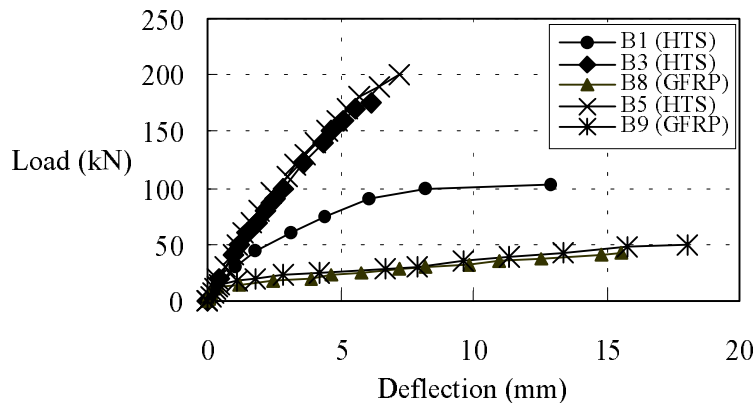

Fig. 6 Effect of type of main reinforcement on the load-deflection relationship

Figure 6 shows that changing the type of main reinforcement from HTS to GFRP while keeping the main reinforcement ratio ($\mu = 0.58 \mu b$), web reinforcement ($\mu = 0.202$) and a/d = 2.5 lead to a reduction of the ultimate load and an increase of the beam deflection. For example, the ultimate loads for Beams B8 and B9, reinforced by GFRP, were approximately less than those for Beams B3 and B5, reinforced by HTS, by 77% and 67.5%, respectively. In addition, the slope of the load-deflection curve reduced from 41.24 kN/mm for Beam B3 to 35.71 kN/mm for Beam B8 and from 45.45 kN/mm for Beam B5 to 34.09 kN/mm for Beam B9. Moreover, the maximum deflection increased for Beams B8 and B9 over that of Beams B3 and B5 by 154% and 150%, respectively. It was observed from Figure 6 that the control NSC Beam B1 had an ultimate capacity less than that of Beam B3 by approximately 46% and higher than that of Beam B8 by 140%. In addition, the control NSC beam B1 exhibited a smaller deflection (80%) compared with the HSC beam B8 reinforced by GFRP rods. The reduction of the ultimate capacity and the increase of deflection for the studied beams reinforced by GFRP rods may be attributed to the use of main reinforcement ratio, $\mu=0.58 \mu b$, which is less than the value ($\mu > 1.4 \mu b$) recommended by ACI 440-2001 [18] for beams reinforced by GFRP bars,

Strains in Longitudinal Main Reinforcement

The strains along the longitudinal main reinforcement and web reinforcement were measured by electrical strain gauges and the full details are recorded elsewhere [12]. In this investigation, the relations between the measured loads and the corresponding strains in main reinforcement were plotted in Figure 7 in order to study the behavior of HSC beams reinforced by GFRP rods. It can be seen from the figure that increasing a/d from 1.5 for Beam B7 to 3.5 for Beam B10 lead to an increase in the strain by 84%. The area under the curve for beams B1 and B8 was approximately 122 kN and 319 kN, respectively. It was noticed that the GFRP rods did not fail during testing and they behave as a linearly elastic material till failure of the beam, which happened after excessive cracking in concrete at tension zone. It is interesting to note that the concrete did not crush at the compression zone because of the flange of the T-beam.
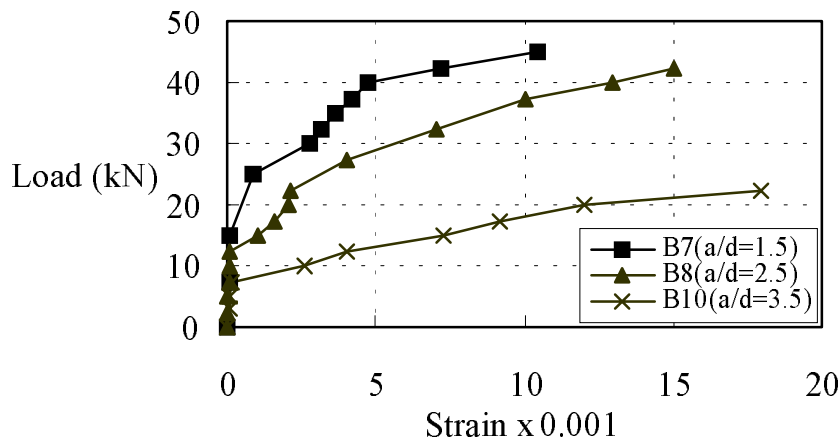

Fig. 7 Load-strain relationship for beams reinforced by GFRP rods.

THEORETICAL PREDICTION OF EXPERIMENTAL RESULTS

Proposed Equation

The ultimate shear capacity of HSC beams reinforced by HTS bars was predicted by an equation developed by Sarsam and Al-Musawi [19]. The authors modified this

equation in order to be applicable for HSC beams reinforced by main reinforcement of GFRP bars as:

$$V_{uPROP} = 1.05\left(f'_c \rho_w V_u d / M_u\right)^{0.38} + A_v f_{yv}/(bS)$$ (N, mm)   (1)

Where f'_c = Cylinder compressive strength of concrete.
ρ_w = Longitudinal steel ratio.
V_u = Factorized shear force at section.
d = Effective beam depth.
M_u = Factorized moment at section.
A_v = Area of shear reinforcement.
f_{yv} = Yield strength of shear reinforcement.
b = Web width.
S = Spacing of shear reinforcement.

Prediction of Test Results using different Codes and Proposed Equation

Shear strength results were predicted by the relevant codes of practice, ACI 318-99 [13], BS- 8110 [20], ECCS 203-2001 [21], to assess the validity of such codes when applied to HSC beams reinforced by GRFP bars as main reinforcement and web reinforcement. Prediction of the test results by the above-mentioned codes of practice and the equation developed by Sarsam and Al-Musawi [19] is listed in Table 4. Table 4 shows that, generally for beams reinforced by HTS, the shear strength predicted by different codes of practice and the equation developed by Sarsam and Al-Musawi [19] was conservative to different degrees. Shear strength predictions using BS- 8110 [20] and the equation developed by Sarsam and Al-Musawi [19] were more accurate than those predicted by ACI 318-99 [13] and ECCS 203-2001 [21]. It can be noticed from the table that increasing a/d and μv lead to enhancing the prediction. For example, the prediction of the results for beam B4 (a/d=3.5) is more accurate than that for beam B2 (a/d=1.5) for all the methods listed in the table. In addition, for the same a/d (2.5), increasing μv from 0.202 for beam B3 to 0.50 for beam B6 resulted in increasing the prediction accuracy for all the methods in a range of 15-27%.

Table 4   Prediction of Shear Strength by Different Codes of Practices and the Proposed Equation

Beam No.	Type of main steel	μv=Av/bS	a / d	$\dfrac{V(test)}{V(ACI)}$	$\dfrac{V(test)}{V(BS)}$	$\dfrac{V(test)}{V(ECCS)}$	$\dfrac{V(test)}{V(PROP)}$
B1	(H.T.S)	0.202	2.5	2.250	1.820	2.595	1.98*
B2	(H.T.S)	0.202	1.5	4.562	2.897	5.382	3.175*
B3	(H.T.S)	0.202	2.5	3.177	2.540	3.748	2.578*
B4	(H.T.S)	0.202	3.5	2.535	2.027	2.990	2.268*
B5	(H.T.S)	0.324	2.5	2.898	2.385	3.333	2.417*
B6	(H.T.S)	0.50	2.5	2.587	2.193	2.900	2.219*
B7	(GFRP)	0.202	1.5	0.947	1.032	1.117	1.618
B8	(GFRP)	0.202	2.5	0.671	0.885	0.791	1.263
B9	(GFRP)	0.324	2.5	0.879	1.110	1.011	1.471
B10	(GFRP)	0.202	3.5	0.552	0.729	0.651	1.104

* Predicted by Sarsam and Al-Musawi equation [19].

For beams reinforced with GFRP bars, the situation was different. The shear strength predicted by ACI 318-99 [13], was not conservative especially for B8 and B10 (with the increase of a/d). BS- 8110 [20] and ECCS 203-2001 [21] were conservative in predicting shear strength for beams B7 and B9 while their trend was similar to ACI 318-99 [13] for beams B8 and B10. Unlike the studied codes, the proposed equation was conservative and more accurate for predicting the shear strength for all the studied beams to different degrees. However, the proposed equation was less conservative with the increase of a/d. For example, increasing a/d from 1.5 for beam B7 to 2.5 for beam B8 lead to a reduction in the over estimated value of shear strength by 22% while increasing a/d to 3.5 for beam B10 resulted in a further reduction (approximately 32%). In addition, the proposed equation was more conservative by 16% with the increase of the web reinforcement ratio, μv from 0.202 for beam B8 to 0.324 for the beam B9.

CONCLUSIONS

Based on the experimental results in this paper, the following conclusions for HSC beams reinforced with GFRP bars can be drawn:

Increasing shear span to depth ratio a/d resulted in the concentration of cracks in the flexural region. Increasing of a/d from 1.5 to 3.5 resulted in reducing the ultimate load capacity of the studied beams by approximately 42%, increasing the maximum deflection by approximately 42% and increasing the strain in the longitudinal main reinforcement by 84%.

Increasing the amount of web reinforcement μv resulted in an increase of the number of cracks and crack width and a reduction of cracks spacing. Increasing of μv from 0.202 to 0.324 resulted in enhancing the ultimate load capacity of the studied beams by approximately 53.0% and increasing the maximum deflection by approximately 16%.

Changing type of main reinforcement from HTS to GFRP lead to changing of the mode of failure from diagonal tension shear failure to flexural failure. In addition, the ultimate capacity of the studied beams dramatically reduced by approximately 73% and the maximum deflection increased by approximately 152%. This may be attributed to the brittleness of HSC compared with NSC and the use of GFRP in reinforcement while keeping the main reinforcement ratio less than the value ($\mu > 1.4$ μb) recommended by ACI 440-2001 [18] for beams reinforced by GFRP bars

Within the limits of the test results of this research, it was found that the proposed equation for predicting the shear strength was more conservative and accurate than the relevant codes of practice for HSC beams reinforced by GFRP bars. The prediction was sensitive to the effect of shear span to depth ratio and the web reinforcement ratio.

ACKNOWLEDGEMENT

REFERENCES

Fumio Watanabe and Jung-Yoon Lee (1998) "Theoretical Prediction of Shear Strength and Failure Mode of Reinforced Concrete Beams "ACI Structural Journal/ November-December.

ASCE-ACI Committee 445 on Shear and Torsion (1998) "Recent Approaches to Shear Design of Structural Concrete "Journal of Structural Engineering/ December.

"State-of-the-Art Report on High Strength Concrete (1997) "Reported by Committee 363, ACI 363R-97.

Michael P. Collins, Denis Mitchell, Perry Adebar, and Frank J. Vecchio (1996) "A General Shear Design Method "ACI Structural Journal / January-February.

Raghu S. Pendyala and Prian Mendis (2000) "Experimental study on Shear Strength of High-strength Concrete Beams "ACI Structural Journal / July-August.

Benmokrane, O. Chaallal, and R. Masmoudi (1996) " Flexural Response of Concrete Beams Reinforced with FRP Reinforcing Bars "ACI Structural Journal / January-February .

Nawy, E.G., and Neuwerth, G. E. (1971) "Behavior of Fiber Glass Reinforced Concrete Beams," Journal of Structural Division, ASCE, September, pp. 2203-2215.

Saadatmanesh, H., and Ehsani, M. R. (1991) "Fiber Composite Bar for Reinforced Concrete Construction," Journal of Composite Materials, V. 25, February, pp. 188-203.

Satoh, K.; Kodama, K.; and Ohki, H. (1991) " A Study on the Bending Behavior of Repaired Reinforced Concrete Beams Using Fiber Reinforced Plastic (FRP) and Polymer Mortar," Evaluation and Rehabilitation of Concrete Structures and Innovations in Design, Proceedings ACI International Conference, Hong Kong, pp. 1017-1031.

Faza, S. S., and GangaRao, H. V. S. (1992) " Bending and Behavior of Concrete Beams Reinforced with Fiber Reinforced Plastic Rebars," WVDOH-RP-83 Phase 1 Report, West Virginia University, Morgantown, pp. 128-173.

Zia, P.; Ahmad, S.; Garg, R.; and Hanes, K. (1992) " Flexural and Shear Behavior of Concrete Beams Reinforced with #D Continuous Carbon Fiber Fabric," Concrete International, V. 14, No. 12, December, pp. 48-52.

Awwad, W. H (2002) "Shear Behavior of Reinforced High Strength Concrete Beams" MSc Thesis in preparation, Faculty of Engineering, Shoubra, Zagazig University.

ACI Committee 318 (1999) "Building Code Requirements for Structural Concrete (ACI 318-99) and Commentary (ACI 318R-99)," American Concrete Institute, Detroit, 369 pp.

Khalil, A. H. H (1994) "Behavior of Concrete Slabs Reinforced With Fiber Glass Rebars "Ain Shams University, M. SC.

Masmoudi, R; Theriault, M; and Benmokrane, B. (1998) "Flexural Behavior of Concrete Beams Reinforced with Plastic Reinforcing Rods "ACI Structural Journal/ November-December.

Johnson M. and Ramirez J. (1989) "Minimum Shear Reinforcement in Beams with Higher Strength Concrete," ACI Structural Journal, V.86, No. 4, July-August, pp.376-382.

Abdoun, S. G. (1998) "Effect of Axial Compressive Stresses on Shear Strength of High Strength Concrete Beams with Web Reinforcement "Cairo University, Ph.D.

ACI Committee 440 (2001) "Guide for the Design and Construction of Concrete Reinforced with FRP Bars," American Concrete Institute, Detroit, May.

Sarsam, Kaiss F. and Al-Musawi, Janan M. S. (1992) "Shear Design of High - and Normal strength Concrete Beams with Web Reinforcement" ACI Structural Journal / November-December.

British Standard Institute (1985) "Structural use of Concrete," Part 1, Code of Practice for Design and Construction, BS 8110, part 1.

"Egyptian Code of Practice and Design for Reinforced Concrete Structures," (2001) Ministry of Housing, Cairo, Egypt, ECCS 203-2001.